Real HBM and MM Waveform Parameters

Jon Barth (1), John Richner(1), Leo G. Henry(2), Mark Kelly(3)

(1) Barth Electronics, Inc., 1589 Foothill Drive, Boulder City, NV 89005 USA
Tel.: +(011)-702-293-1576; Fax: +(011)-702-293-7024; e-mail: jonbarth@ieee.org

(2) ESD/EMI/TLP Consulting, P.O. Box 1665, Freemont, CA 94538 USA
Tel.: +(011)-510-657-5252; Fax: +(011)-510-657-9661; e-mail: leogesd@pacbell.net

(3) Delphi Delco Electronics Systems, P.O. Box 9005, M/S R117, Kokomo, IN 46904-9005 USA
Tel.: +(011)-765-451-7084; Fax: +(011)-765-451-9647; e-mail: mark.a.kelly@delphi.com

Abstract - Recent "real" HBM and MM discharge waveform measurements provide completely new data on the risetime and peak current threats to devices. Additional investigations were performed to determine impact of humidity and electric field effects on the discharge event. Given the new information, redesign of ESD simulators and development of test standards representing real-world ESD threats are essential.

I. Introduction

The basic premise of this paper was developed from measurements to identify actual dI/dt rates for ESD discharges defined in the Human Body Model (HBM) and Machine Model (MM) test standards [1,2]. Despite recent advancements in technology, the dI/dt and peak current waveform parameters defined many years ago for HBM and MM testing have remained unchanged. Measurements reported in "Correlation Considerations II: Real HBM to HBM Testers", presented at the EOS/ESD Symposium in 2002 [3] found that real HBM (produced by a charged human finger touching a device pin) produces much faster rates of rise than those specified in the test standard. Real HBM was also identified as having a highly variable exponential decay waveform.

To expand on the results of 2002 [3], additional discharge measurements were conducted to determine the impact that air humidity and non-uniformity of the spark gap electric field may have on the actual discharge waveform. To determine how the spark would be affected when a finger discharged to a device pin or PC board on which a device is mounted, a sharp contact was added to the current sensor. This created higher spark resistances, resulting in lower peak currents and slower rates of rise.

Measurements involving real-world MM revealed a completely different waveform than what is specified in the MM test standard, most importantly a fast rate of rise similar to real HBM. Although most MM simulators incorporate inductance to meet test standard waveform requirements, an inductor should not be used as the first wave shaping element. This inductor, which slows the rise time, also creates a sine wave discharge that does not simulate real MM discharge waveforms. True MM is closer to a cosine waveform. As stated in previous work [3], measurements of real-world HBM show that the exponential decay is not constant, but rather has a constantly varying exponential after the initial peak current. An analysis is presented on the effect of rapidly increasing spark resistance during the discharge event and how it can reduce the peak temperature heating threat that ultimately damages protection circuitry. New findings will show ESD protection circuit designers that the dV/dt rates currently being used for design and analysis should be modified in order to survive both standardized ESD test methods and real-world threats.

II. Improved Measurement Capability

High speed oscilloscopes (6 GHz bandwidth, 60 ps risetime capability) have recently become available, allowing for measurements that accurately characterize the fastest spark discharges. Aside from 50 V Machine Model discharges (with risetimes faster than 60 ps), the measurements accurately captured the risetimes. Although low voltage HBM measurements

have been performed on discharges with risetimes as fast as 50 ps [3,4], parasitic inductance and capacitance inherent to device packages often slow a fast rate of current rise when passing through a device during test.

Real ESD discharge risetimes, while impossible to accurately measure when HBM standards were being developed [5], can now be easily and accurately measured with high speed oscilloscopes. Measurements were made using a Tektronix TDS 6604 Digital Storage Oscilloscope with a risetime capability of 60 ps and a BEI Model 4603 current sensor with a clean risetime response of 35 ps. A three-foot piece of low loss 3/8-inch diameter Semflex coaxial cable was used to carry the current pulse from the current sensor to the digitizing oscilloscope with minimum distortion. This methodology allows for an accurate analysis of the discharge event and a more precise analysis of how those events affect ESD protection circuitry and the interaction with ESD simulators.

III. Real HBM Discharge Measurements

Measurements presented in 2002 [3] showed high peak current values with sub-nanosecond risetimes. We repeated these measurements using a 60 ps risetime oscilloscope to provide additional risetime and peak current data beyond the capability of previous equipment. Figure 1 illustrates a typical real HBM waveform.

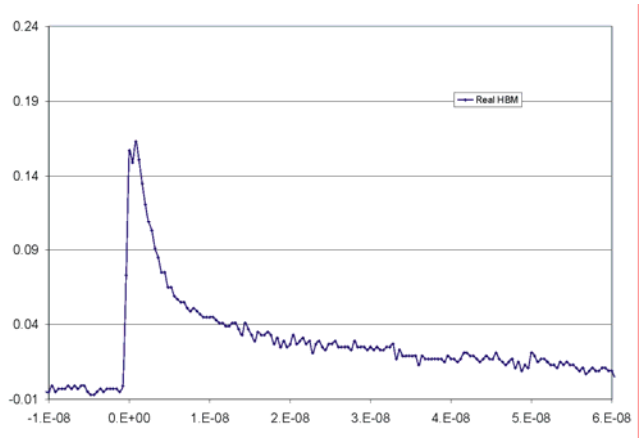

Figure 1. Real HBM Discharge Current Waveform.

We also determined the effect of higher humidity and non-uniform fields on real-world HBM discharge events. The previous data was collected at 10 % relative humidity with a uniform electric field spark gap and generated waveforms from human "volunteers" charged to levels between 1 kV to 6 kV and then discharging into the current sensor and 2 GHz oscilloscope [3]. Over 50 real HBM discharge measurements were obtained using the faster 6 GHz oscilloscope with the 2002 [3] current sensor and faster risetime values were observed. The rising edge of real HBM discharge events is quite different from what is described in the test standards. This is important because the dV/dt parameter is not specified or simulated in present HBM/MM test methodology and occurs just as the protection circuitry is triggered.

A. Humidity Effects on HBM

During measurements of high intensity and fast rate of formation discharge events in dry air, moisture content was found to have an impact on the formation and resistance of ESD sparks. An Increase in air humidity from 10 % to 34 % produced a slower spark formation and an increased resistance. The resulting discharge event exhibited a reduced peak current and longer pulse duration than that generated by HBM testers. Figure 2 compares results of typical peak current and risetime measurements for both dry and humid uniform field discharge.

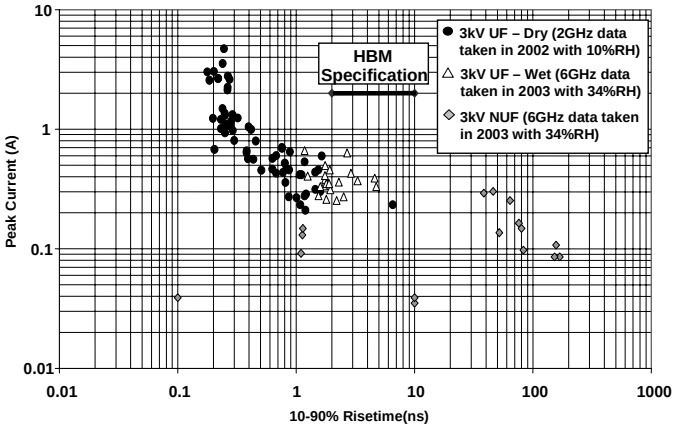

Figure 2. Real HBM at 3kV, previous data versus Uniform and Non-Uniform Field data.

Cold air (0 °C) with high moisture content that is warmed to 68 °F (20 °C) will only retain small amounts of water, unless it is artificially humidified. Therefore, the greatest discharge threats occur in dry air environments (e.g., during cold weather conditions in temperate climates or year-round in dry desert air). In areas using air conditioning, the effect is a removal of air moisture to increase the comfort level, thereby drying the air and increasing both the speed and intensity of an HBM discharge event. Another method of altering moisture content in air known as swamp cooling (commonly used in desert conditions), where moisture content is increased, reduces not only

the HBM threat level but also the severity of the discharge. Real HBM measurement obtained during a few rainy days in Nevada resulted in higher resistance and slower risetime HBM spark conditions, compared to results from our typical dry days, all shown in Figure 2.

B. Non-Uniform Field Effects on HBM

Until now, measurements were focused on Uniform Field (UF) HBM discharge events (see Figure 3).

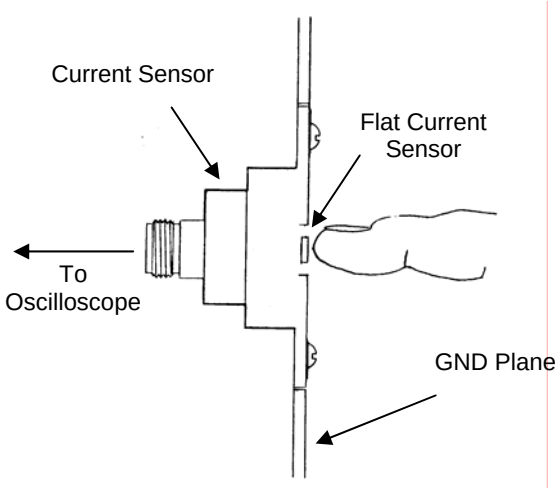

Figure 3. Uniform Field Contact on Current Sensor

However, spark characteristics can be affected not only by humidity but also by Non-Uniform Fields (NUF). Non-uniform fields exist when the human finger is discharged to a sharp pin of an IC or to a thin copper trace leading to an IC. Additional data was gathered using a pointed metal contact attached to the current sensor (see Figure 4) to generate non-uniform field gradients.

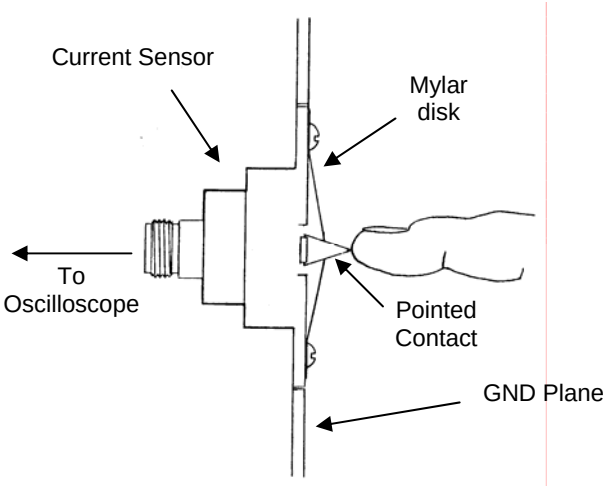

Figure 4. Non-Uniform Field Contact on Current Sensor.

This modification for NUF measurements maintained the 0.5 V per amp sensitivity of the BEI Model 4603 current sensor. The pointed metal contact is compressed against the uniform field contact disk by a large Mylar disk placed under four plastic screw heads, as shown in Figure 4, to minimize field distortions.

NUF measurements performed at 34 % humidity resulted in a slowed discharge risetime, increased spark resistance, and greatly decreased peak discharge currents. Calculations of the spark resistance using measured peak current and charge voltage levels revealed typical values of 20 kΩ to 100 kΩ! However, the highest peak current for a 1 kV charge voltage was a mere 0.14 A, equating to an initial spark resistance of 7 kΩ.

The measured peak current levels were so low that they constitute minor ESD threats. However, the long discharge time from high resistance sparks allows the voltage to remain across the ESD protection circuitry (including the gate oxide) for a much longer duration than that from HBM simulators.

IV. Real MM Discharge Measurements

Given the observed limitations of the HBM standard (e.g., dV/dt parameter not representative of real HBM) and the test methodology similarities between HBM and MM, the MM standard also came under scrutiny. Basic measurements were performed to study the initiation of ESD sparks at low voltages of 50 to 200 V. Because real-world "machines" are required to be properly grounded in a device handling application, evaluation of ungrounded "machines" was difficult. To accomplish this task, machines were constructed using both open metal box frames (all sides open) and enclosed solid metal box frames. Measurements were obtained by charging the representative "machine" to a given voltage level and discharging into the same high speed current sensor configuration used for real HBM measurements (see Figure 5).

Figure 6 illustrates a typical discharge waveform from an enclosed frame (six sided, rectangular metal frame with dimensions of 18" x 20" x 14"). Figure 7 illustrates a typical discharge waveform from an open frame (rectangular metal frame with dimensions of 21" x 19.5" x 12.5", no sides). Although significant variations in "wave shape" were observed, the real MM discharges for several open and enclosed metal frames revealed very fast rates of rise (from ground to

at least half of the peak amplitude) followed by a highly damped rectangular/sinusoidal ringing decay. Based on these observations, the real MM discharge waveform is better described as a cosine waveform, due in part to the sinusoidal portion of the waveform decay beginning near the peak amplitude.

Figure 5. Photo of real MM test configuration (using 18" x 40" x 14" enclosed frame).

As shown in Figures 6a and 7a, discharges from open and enclosed frames (recorded at 20 ns per division) produced similar waveforms. The leading edge was then expanded in time at 400 ps per division, in the digitizer as shown in Figures 6b and 7b. The initial real MM measurements suggest that the overall size of a "machine" determines the primary pulse width and amount of energy stored in the waveform. The most obvious fact from these MM discharges is that both machine types had immediate and fast rising cosine waveforms, which is quite different from the MM standard waveform specification.

The MM threat, especially those below 300 V, is likely initiated by emission [6-10] and is extremely fast, often times faster than the capability of most measurement equipment. Measurements at charging levels of 50 to 200 V were extremely fast and, as expected, some exceeded the capability of the 60 ps risetime oscilloscope. As mentioned earlier, the MM discharge waveform is determined by the dimension and shape of a "machine", and its relation to the ground plane return path. The observed discharge has an approximate rectangular shape, affected by the given length of the machine and due in part to an approximate transmission line with an unmatched load resistance between the spark and one-ohm current sensor. The impedance of the machine (relative to the ground plane return path) conducts current into the low resistance spark and zero resistance ground plane. The resulting mismatch between 1) the spark resistance and one-ohm current sensor and 2) the impedance of the machine and ground plane, generates reflections that travel back and forth along the machine (similar to a transmission line).

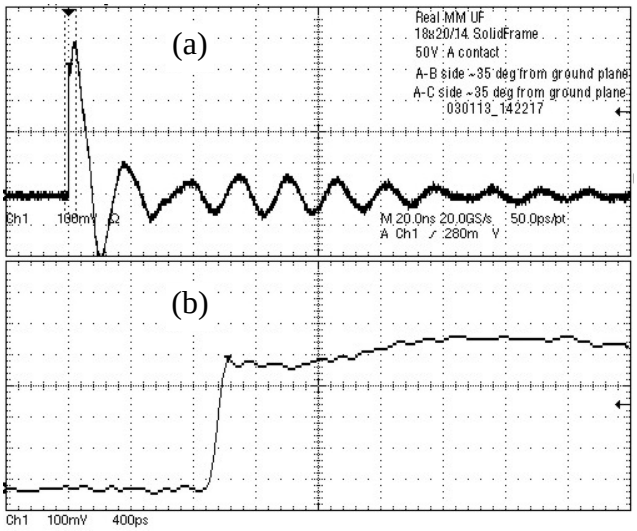

Figure 6. Enclosed "machine", Real MM Discharge, Uniform Field, Timescales of (a) 20 ns per division and (b) 400 ps per division.

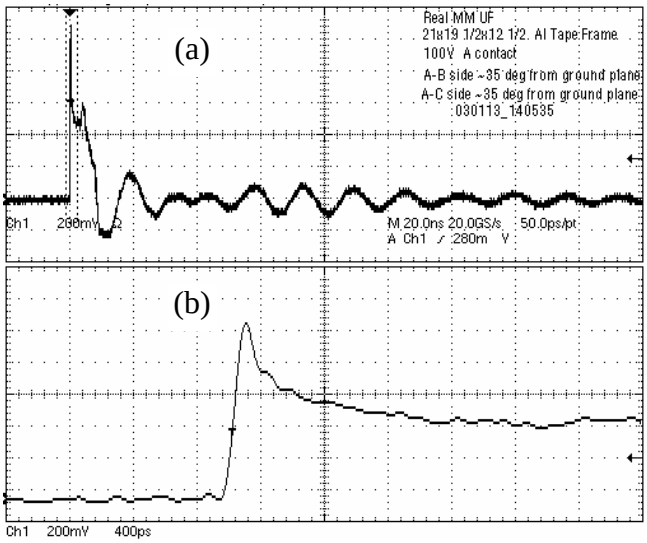

Figure 7. Open "machine", Real MM Discharge, Uniform Field, Timescales of (a) 20 ns per division and (b) 400 ps per division.

The sine wave ringing has a decreasing amplitude as energy is radiated from the "machine" and dissipated in the spark. The amplitude observed for the initial pulse is much larger than that found in the secondary ringing. Therefore, the energy in the first pulse can be many times that of the sine-wave ring down that follows, as shown in figures 6 and 7. Observations

indicate that the discharge current will demonstrate some ringing after the initial pulse and it occurred more often when one side or edge of the machine was nearly parallel to the ground plane, thus forming a bulky transmission line discharge.

Unlike the real HBM results, MM discharges are only slightly affected by humidity, a slight slowing and minor increase in resistance due to the spark discharge formation in the short gap at low voltages. Metal to metal conditions for initiation are very different from HBM. A "machine" with a relatively sharp metal corner actually has a radius that is quite large when compared to the short spark gap spacing during low voltage discharge events. This minimizes the effect of the sharp metal conductors and produces a more uniform electric field in the spark gap.

V. HBM Spark Discharge Analysis

Spark formation velocity and breakdown voltage in air have been studied in detail for quite some time [5,11,12]. For real HBM, our results indicate that the spark resistance is the primary variable affecting the discharge event. The resistance of a spark current channel discharge is inversely proportional to the degree of ionization; therefore, spark channel resistance decreases with an increasing degree of ionization.

Non-uniform field gap length is usually longer than that for a uniform field, as less voltage is required to initiate a spark in a non-uniform electric field gap. Longer sparks need more time to bridge the gap and therefore result in slower risetimes. The non-uniform electric field also results in an increased spark resistance (due to the discharge formation generated by a metal device lead or sharp metal edge of a PC board).

Early HBM test specifications seem to be based on very few real HBM discharge measurements made with limited risetime-capability equipment (when compared with equipment available today). It is also unlikely that early measurements performed an analysis of the high rate of discharge, as discussed in this paper and in, the paper of 2002 [3]. Those early test specifications, based on inexact data, are still in use today. The present discharge measurements of real HBM threats provide better insight, improved data on the real threat, and can be used to more closely simulate real HBM threats. The spark discharge in air is one of the most complex phenomena in gas discharge physics. Therefore, real-world ESD discharge events are better characterized by measurement than by theoretical explanations.

There are two easily identifiable variables affecting spark formation. The first variable is humidity, or the amount of water dissolved in the air. Measurements indicate an increase in humidity result in an increased spark resistance and a slower rate of current risetime. The second variable relates to non-uniform gap electric fields, also resulting in an increased spark resistance and a slower discharge risetime. If one spark gap electrode has a radius that is much smaller than the distance to the other electrode, a non-uniform field is generated; however in a very short gap the electric field becomes more uniform.

A. Spark Discharge 1/e Variations

Although measurements indicate real HBM peak current values exceed those defined in test standards, an attempt was made to equate the two versions. A real HBM discharge consists of three regions: 1) an initial impulse with a fast decay, 2) a slower decaying exponential middle region that typically lasts 10 to 20 ns, and finally 3) an ending region with an even slower exponential decay. It soon became clear, during these measurements, that real HBM events have multiple exponential decay values, and the very narrow peak current was significantly different from the test standard. The variability in exponential decay is a function of the spark resistance, which is at its lowest value when peak current first occurs but rapidly increases throughout the remainder of the discharge event. More recent analysis indicates that the initial sub-nanosecond wide impulse portion is probably caused by a transmission line effect in the hand and arm, and may be studied in detail in a future paper. Knowing that the variability in exponential decay is a function of the spark resistance, we can understand why the same peak current generated by a real HBM event and one from an HBM simulator will not produce the same pulse energy in the device. This difficulty led us to further analyze the real HBM event and determine the underlying cause of the variable exponential shapes.

While measuring high current intensities and fast rates of spark formation in dry air, we observed that the fastest discharges most often had the highest peak current values that rapidly decayed within a few nanoseconds. It was also noted that humid air slowed the spark formation, resulting in limited peak currents and much higher spark resistance values. These "high moisture" discharges did not possess the rapid peak current decay observed with dry air discharges, as the spark resistance started at a high value and then also increased, but much less dramatically. The result is an exceptionally long waveform current decay,

significantly longer than that of the HBM test standard, but generally, also posing a lesser threat to the device.

The decaying portion of all real HBM waveforms has a varying exponential component and is quite different from the HBM test standard specification. The rate of decay following the peak current amplitude is affected by a widely changing spark resistance throughout the entire decay time. At the point when peak current is achieved, the spark resistance is at its minimum value. As the current decreases and the stored energy is discharged, the spark resistance increases. Since real HBM, with its constantly changing decay exponent, differs significantly from that produced by an HBM simulator, direct comparison of these waveform types is extremely difficult and confusing.

The typical real HBM discharge in dry air shown in Figure 1, with its relatively high peak current and fast risetime, illustrates the multiple exponential decay regions for the single discharge event. Figure 8 shows the same discharge waveform along with three different single exponent discharge waveforms, one for each region of the discharge event. The EXP 1 waveform was calculated to have the same decay rate found in the first 3 ns of the real HBM discharge. Next, EXP 2 was calculated to have the same decay rate found in the next 15 ns. Finally, EXP 3 was calculated to have the same decay rate found from 20 to 60 ns. The three different plots show that a real HBM discharge is not a single exponential discharge; but has a constantly varying decay rate. The high current, short impulse shown on the leading edge of the waveform is most likely due to the variation in spark resistance with only a minor contribution from lossy human arm or body transmission line effect.

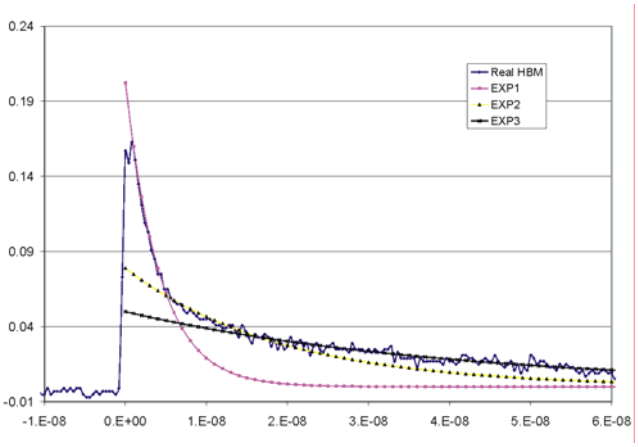

Figure 8. Exponent Decay regions of Real HBM.

B. Effect of Energy/Time

The primary damage mechanism to silicon ESD protection structures is heat generated by energy dissipation. Applying a single exponentially decaying current pulse to protection circuitry produces a peak temperature value (where the heat buildup from the decaying current is equal to that lost by thermal conduction) well after the peak current has been reached. The heating resulting from the exponentially decaying current waveform peaks at a predictable time, is repeatable, and is dependent on both the volume of silicon being heated and the thermal conductivity removing heat [13,14,15].

Unfortunately, the peak current of real HBM discharge cannot be compared to that of the simulator because the decay waveforms are very different. Once the peak current is reached, the rate of decay for real HBM discharges is controlled by both the human body capacitance and the spark discharge resistance. The human body capacitance remains constant during the discharge; however, measurements clearly show that the spark resistance immediately following the peak current increases significantly. While the spark resistance begins at a low value that determines the peak current; it increases rapidly as the current through the spark decreases. This results in significantly lower current throughout the remaining real HBM discharge and an increase in the total time to completely discharge.

Currently available digitizing oscilloscopes, used in measurement of real HBM discharge waveforms, can easily perform relative power calculations using waveform data points. Integration of these points over the total discharge time can then provide energy for the given discharge. These values can also be used to calculate peak temperature in the silicon and estimate when it will occur. The results can ultimately be used in the comparison between real-world HBM threats and those generated by ESD simulators.

The purpose of ESD testing is to determine the capability of protection circuitry to survive an ESD discharge event. Thus, ESD protection circuitry and the spark must dissipate the total discharge energy during a specified time, while experiencing temperature increases until the event subsides or damage occurs. Given that real HBM spark resistance is significantly higher than the fixed 1500Ω resistor specified for HBM testing, silicon temperatures resulting from the two methodologies will be significantly different. The real HBM discharge with the faster decaying current will create a lower

temperature in the silicon than the more slowly decaying HBM simulator pulse, even though both have the same peak current. These temperature differences can cause different failure levels.

VI. IVR Rates

The voltage where a snapback device begins to conduct current is commonly identified in TLP parlance as the Vt1 point. This is where the circuit turns on and begins to provide protection. In 2002 [3], the term Initial Front Rise (IFR) was introduced to identify the voltage rate of rise that triggers, or turns on, device ESD protection circuitry [3]. This dV/dt parameter is far more important than the 10% to 90% current risetime specification that has been in use for many years. With newer protection circuitry and their inherent sensitivity to dV/dt rates of rise, further investigation was merited. A more meaningful and descriptive term was needed to emphasize the voltage rate of rise and its impact on protection circuitry, thus the slight change in name to Initial Voltage Rise (IVR).

In devices with dV/dt sensitivity, different rates of rise (in the critical 0 to 5V, 0 to 10V, or 0 to 15V turn on range) can affect the Vt1 point and force an ESD threat to take unanticipated current paths within protection circuitry. Unfortunately, ESD test standards concentrate on the 10 % to 90 % rise of current (or dI/dt rate), rather than focusing the more important voltage rate of rise that triggers protection elements. While HBM and MM events are referred to in terms of thousands or hundreds of volts, respectively, protection circuitry is triggered at much lower voltage levels to limit further voltage increases. To resolve this confusion, the IVR rate for HBM/MM simulators and real-world HBM/MM threats must be understood. While devices can be exposed to real-world IVR threats throughout its life, present ESD simulators (with emphasis on a 2 to 10 ns current waveform risetime specification) are unable to deliver real-world dV/dt rates. Thus, a more precise dV/dt specification for ESD testing is needed. More importantly, IVR rates are critical and circuit designers must consider this during design simulation and testing to protect devices against real-world ESD threats, as well as being able to pass HBM testing.

VII. Risetime - The Wrong dV/dt Parameter

Given the fact that present test standards misapply dI/dt risetime specifications rather than focus on the more relevant dV/dt rate, one would expect discrepancies between ESD testing and field performance data. However, HBM testing at excessive levels may prevent failures at lower level real HBM threats with different dV/dt rates of rise. To avoid miss-diagnosing potential ESD sensitivities, the rate of rise parameter for both HBM and MM testing may need further investigation.

ESD spark discharges below 10 kV have very small channel diameters and an inductance of no more than a few nanohenries. The overly simplistic decision by simulator manufacturers to use a 5 to 10 μH inductor in an attempt to slow the discharge risetime was made when ESD threat concerns were not well known and silicon structures were physically much larger. The introduction of this inductor and its parasitic capacitance was used to slow the HBM test pulse and minimize ringing on high pin-count testers. Although it had minimal impact on the IVR rate to the Vt1 point, it was a particularly bad choice because it caused HBM testing to deviate further from simulating real HBM threats. We now understand the 10-90% current risetime to be a less important factor now that IVR has been identified as the critical dV/dt parameter. Redesign of HBM and MM simulators to produce real-world ESD waveforms and development of new meaningful test standards are essential. Now that real-world waveforms have been accurately identified, the time to implement these changes is fast approaching.

VIII. TLP Can Simulate ESD Threats

Real HBM and real MM threats may have subnanosecond IVR rates of rise and designers often use fast dV/dt rates in simulations. However, neither HBM nor MM simulators have ever addressed the IVR rate of rise parameter for device turn on. Designers need to be aware that the real dV/dt threats to the Vt1 point may be faster than what ESD simulators provide. A final measurement method of the IVR when testing snapback type protection is being designed.

Although devices are not required to be tested to this missing parameter, TLP can provide a range of controlled dV/dt rates in the critical IVR portion of a waveform. Using it to evaluate designs provides knowledge of how any circuit will perform to any dV/dt threat. It can directly provide real HBM failure threshold data and exercise circuitry in a manner similar to real MM threats.

The HBM test socket board capacitance provides inherent slowing of the simulator pulse to the Vt1 point. Real HBM does not have this test board capacitance, which stores energy until Vt1 is reached and then dumps that energy into the protection circuit with minimal current limiting resistance. This extra discharge is also not found in TLP. However, placing a capacitor in parallel with the DUT during TLP testing simulates the unavoidable HBM test board capacitance. This methodology and testing at different rates of rise can help identify the cause of differences in failure levels between different HBM simulators. This problem is occurring more frequently and some clear solutions are now becoming available.

IX. Conclusion

The degree of air humidity and electric field uniformity both have a tremendous effect on ESD spark discharge risetime and peak current intensity. ESD generated in a dry air, uniform field environment results in the greatest peak current and fastest risetime values, and likely pose the greatest threat.

Measurements of real HBM discharge events generated in humid air (>30% RH) and with a non-uniform field revealed risetime values ranging from 0.1 to 100 ns. The fastest real HBM discharges exhibited an impulse or spike at the leading edge of the waveform and a very fast decay rate, which differs significantly from present HBM test standards. Results also indicate that, for a given voltage, the energy density of real-world HBM discharges is spread over a much longer duration than that of present HBM standards.

Real MM events were captured using simple "machines" constructed using metal frames or boxes. Observations of these real MM discharges revealed a cosine waveform, as opposed to the MM test standard sinusoidal waveform. Real MM events also exhibited extremely fast risetimes with a flat or rounded peak occasionally followed by a smaller damped ringing waveform.

TLP can provide a range of controlled dV/dt rates in the critical IVR portion of a waveform, a parameter that is uncontrolled in present HBM and MM test standards. Now that real HBM and MM threats have been shown to have sub-nanosecond rates of current rise, TLP testing can provide circuit designers with a means to examine protection circuitry I-V characteristics for different dV/dt rates.

Results from real HBM and the simulated real "machine" discharge measurements provide insight as to the real-world threats that devices may experience throughout their life. This information is now available for comparisons to present test standards. Measurements of real-world HBM and MM threats provide improved data to serve as the foundation for developing test standards that more closely simulate real HBM and MM threats.

Acknowledgements

The authors want to thank MK Radhakrishnan for his careful review and guidance. Our late friend and colleague, Hugh Hyatt, would have been a valuable ally in this attempt to improve test standards. Hugh's experience in time domain measurements and his constant search to improve test methods will be greatly missed as this work continues.

References

1. "ESD-STM5.1-2001," ESD Association Standard Test Method for Electrostatic Discharge (ESD) Sensitivity Testing – Human Body Model (HBM) – Component Level, 2001.

2. "ESD-STM5.2-1998," ESD Association Standard Test Method for Electrostatic Discharge (ESD) Sensitivity Testing – Machine Model (MM) – Component Level, 1998.

3. J. Barth, J. Richner, K. Verhaege, M. Kelly, L.G. Henry, "Correlation Considerations II: Real HBM to HBM Testers", EOS/ESD Symposium Proceedings EOS-24, pp. 155-162, 2002.

4. J. Barth, D. Dale, K. Hall, H. Hyatt, D. McCarthy, J. Nueble, D. Smith, "Measurements of ESD HBM Events, Simulator Radiation and Other Characteristics Toward Creating A More Repeatable Simulation or; Simulators Should Simulate", EOS/ESD Symposium Proceedings EOS-18, pp. 211-222, 1996.

5. M.A. Kelly, G.E. Servais, T.V. Pfaffenbach, "An Investigation of Human Body Electrostatic Discharge", Proceedings of the 19th ISTFA (International Symposium for Testing and Failure Analysis), pp. 167-173, 1993.

6. A. Wallash and L. Levit, "Electrical Breakdown and ESD Phenomena for Devices with Nanometer -to-Micron Gaps", Proceedings of Reliability Testing and Characterization of MEMS/MEOMS II, SPIE Conference, Paper 4980-10, 2003.

7. R.M. Schaffert, “Electrophotography”, John Wiley & sons, pp. 514-517 (1975) and Focal Press Limited Version, pp. 319-23 (1965).

8. R.H. Fowler & L. Nordheim, “F-N Theory on Field Emission - Tunneling”, Proc. Roy. Soc. (London), A119, pp. 173 (1928) and A124, pp. 699, (1929).

9. R. Gomer, “Field Emission and Field Ionization”, Harvard Univ. Press, 1961 and American Institute of Physics, 1993.

10. A. Wallash, “ESD Challenges in Magnetic Recording: Past, Present and Future”, IRPS Proceedings, pp. 222-228, 2003.

11. E.M. Bazelyan and Yu. P. Raizer, “Spark Discharge”, Sections 1, 2, 3, & Supplement A; CRC Press LLC, 1998.

12. H. Hyatt, "The Resistive Phase of An Air Discharge and the Formation of Fast Risetime ESD Pulses", EOS/ESD Symposium Proceedings EOS-14, pp 55-67, 1992.

13. D. Lin, “Thermal Breakdown of VLSI by ESD Pulses”, IRPS Symposium Proceedings, pp 281-287, 1990.

14. K. Verhaege, C. Russ, D. Robinson-Hahn, M. Farris, J. Scanlon, D. Lin, J. Veltri, G. Groeseneken, “Recommendations to Further Improvements of HBM ESD Component Level Test Specifications“, EOS/ESD Proceedings EOS-18, pp 40-53, 1996.

15. P. Salome, C. Leroux, P. Crevel, J.P. Chante, “Investigations on the Thermal Behavior of Interconnects Under ESD Transients Using A Simplified Thermal RC Network”, EOS/ESD Proceedings EOS-20, pp 187-198, 1998.